

# Properties of SiO<sub>2</sub> and Si<sub>3</sub>N<sub>4</sub> layers deposited by MF twin magnetron sputtering using different target materials

M. Ruske<sup>a,\*</sup>, G. Bräuer<sup>a</sup>, J. Pistner<sup>a</sup>, J. Szczyrbowski<sup>a</sup>, M. Weigert<sup>b</sup>

<sup>a</sup>LEYBOLD SYSTEMS GmbH, Wilhelm-Rohn-Strasse 25, D-63450 Hanau, Germany

<sup>b</sup>LEYBOLD MATERIALS GmbH, Wilhelm-Rohn-Strasse 25, D-63450 Hanau, Germany

## Abstract

Si<sub>3</sub>N<sub>4</sub> and SiO<sub>2</sub> layers can be deposited by reactive sputtering in a stable manner by using MF twin magnetron systems. The increasing demand for these materials for industrial applications makes it necessary to find new solutions for the target material. The up to now mostly used boron-doped poly-crystalline silicon suffers from serious drawbacks. In this paper, properties of Si<sub>3</sub>N<sub>4</sub> and SiO<sub>2</sub> layers deposited by using casted Si/Al alloy targets as well as conventional Si targets are compared. The advantages of using casted alloy targets are presented. © 1999 Elsevier Science S.A. All rights reserved.

**Keywords:** Optical coatings; Silicon oxide; Silicon nitride; Sputtering; Sputter targets

## 1. Introduction

Since the introduction of MF (sine wave) powered twin magnetron sputter systems, highly insulating dielectrics such as Si<sub>3</sub>N<sub>4</sub> and SiO<sub>2</sub> can be deposited in a stable process [1–3]. The demand for silicon targets for reactive sputtering of these materials is dramatically increasing [1]. Mainly the usage of SiO<sub>2</sub> layers in antireflective coating systems and the application of Si<sub>3</sub>N<sub>4</sub> layers in modern low emissivity layer stacks require large amounts of reliable sputter targets at low cost for the end user [4,5].

Especially with the increased number of planar MF twin magnetron systems (e.g. LEYBOLD TwinMag<sup>®</sup>) installed in mass production lines, the necessity of a more economic solution for flat sputter targets becomes urgent. Up to now practically all planar silicon cathodes were working with boron doped high purity silicon targets [6]. These sputtering targets were produced from large blocks of polycrystalline, so called ‘solar silicon’. This material was 99.999% pure silicon with a boron doping of a few ppm to achieve sufficient conductivity for DC sputtering. Because of the complicated cutting and grinding processes for this target material and because of the necessity of solder bonding of these targets, the target costs for reactive sputtering of silicon compounds in mass production were comparably high. Another disadvantage of the high purity silicon is the high

danger of target cracking as soon as the target is exposed to permanent thermal cycling. This target cracking can cause undesired particle generation in the sputter chamber.

This paper investigates a new class of less brittle and less expensive silicon alloys. These new alloy targets (SISPA<sup>™</sup>, LEYBOLD MATERIALS) promise to overcome the economical, logistical and technical problems with the conventionally used high purity silicon targets.

## 2. Experimental

The SISPA<sup>™</sup> alloys [7] are silicon based with aluminum as major alloying component. With respect to the major alloying components the target material has a purity of 99.9%. The microstructure of SISPA<sup>™</sup> can be seen in Fig. 1. A finely dispersed grain structure of a primary Silicon phase is surrounded by a ductile second phase to minimize the brittleness of the target material.

The SISPA<sup>™</sup> alloys have to be melted under vacuum and they are cast into near net shape molds. The chemical homogeneity and the fine grain dispersion is achieved by very rapid cooling and by the addition of grain refining additives (<0.1%). Because of its good ductility the alloy can be machined easily into any desired planar target geometry.

The essential characterizing data of the SISPA<sup>™</sup> target material are listed in Table 1. The major differences in comparison with pure silicon are a much lower electrical resistance, a slightly higher coefficient of thermal expansion and a lower bending strength and thus less brittleness.

\* Corresponding author. Tel.: +49-618-134-1143; fax: +49-618-134-1850.

E-mail address: ruskemanf@leybold-systems.de (M. Ruske)

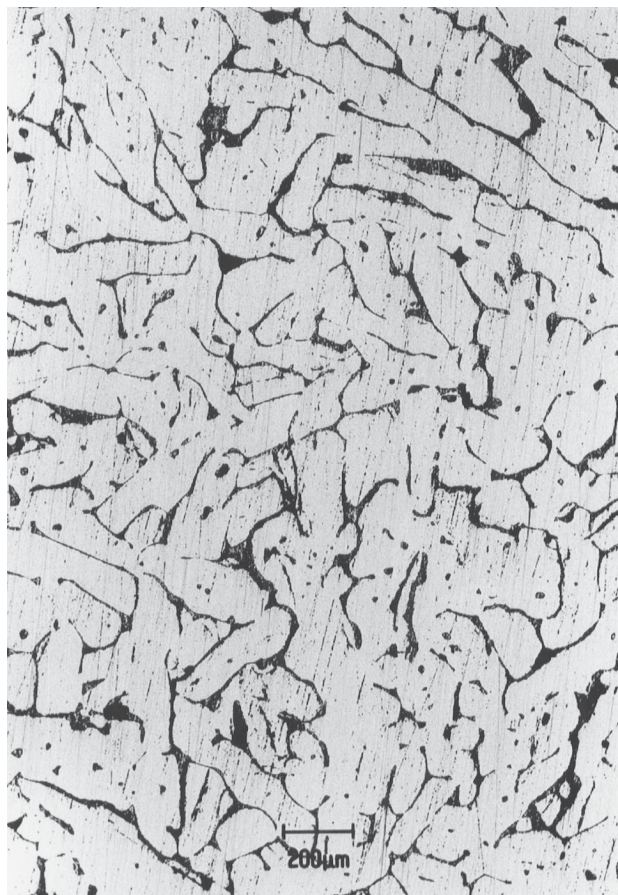


Fig. 1. Microstructure of a SISPA™ 10 alloy target.

During sputtering from a SISPA™ alloy, a much rougher target surface than known from the pure silicon will develop (see Fig. 2). Because of this rough surface, the  $\text{Si}_3\text{N}_4$  or  $\text{SiO}_2$  redeposit at the target edges is sticking much better to the target, thus reducing the amount of particles falling down. Another interesting feature is the possibility to produce clamp versions of the target, which makes it very easy to recycle the used targets. Also larger target tiles can be casted compared to the  $100 \times 100 \text{ mm}^2$  standard size of solar silicon.

$\text{SiO}_2$  and  $\text{Si}_3\text{N}_4$  single layers have been deposited in a

Table 1  
Material data of Si/Al ( $\approx 10 \text{ at.}\%$ )-alloy (SISPA™ 10) in comparison to boron-doped pure silicon

	SISPA™ 10	High purity B-doped poly-Si
Purity (%)	99.9	99.999
Melting point ( $^{\circ}\text{C}$ )	580–1360	1414
Density ( $\text{g}/\text{cm}^3$ )	2.31–2.36	2.33
Grain size (mm)	< 1	10–100
Thermal conductivity ( $\text{W}/\text{m K}$ )	90	126
Electrical resistivity $\Omega \text{ cm}$	$1.4 \times 10^{-4}$	0.5–5
Thermal expansion, $/\text{K}$ ( $100^{\circ}\text{C}$ )	$4.1 \times 10^{-6}$	$2.6 \times 10^{-6}$
Bending strength (MPa)	$38 \pm 3$	$145 \pm 25$

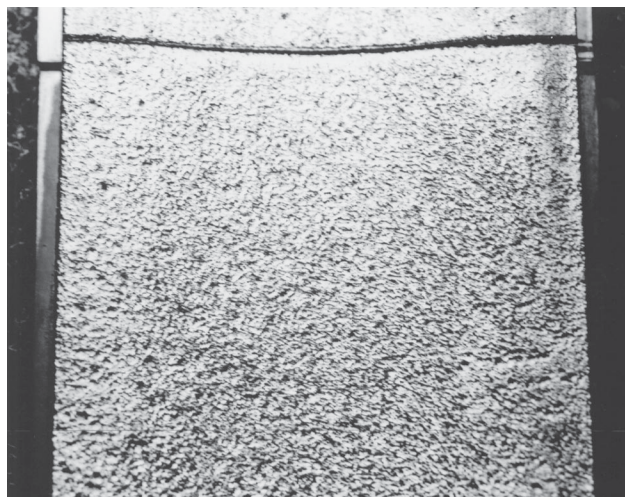


Fig. 2. Surface of a sputtered SISPA™ 10 alloy target.

Leybold Z600 coater using three different target materials: conventional B-doped poly-Si, Si/Al ( $\approx 5 \text{ at.}\%$ ) alloy (SISPA™ 5) and Si/Al ( $\approx 10 \text{ at.}\%$ ) alloy (SISPA™ 10). The used target plates had a size of  $488 \times 88 \text{ mm}^2$ . Two cathodes, each equipped with the target plates, were arranged side by side and powered with a MF sine wave power supply at a frequency of 40 kHz. The applied power density to the target surface was about  $5 \text{ W}/\text{cm}^2$ . The residual gas pressure was about  $3 \times 10^{-4} \text{ Pa}$ . For the deposition of  $\text{SiO}_2$  and  $\text{Si}_3\text{N}_4$ , an Ar/ $\text{O}_2$  and Ar/ $\text{N}_2$  gas mixture was used, respectively. The total gas pressure was varied between 0.15 and 1.2 Pa. The flow of the reactive gas component was adjusted to obtain fully transparent layers at the highest possible deposition rate. Slide glass with a thickness of 1 and 3 inch Si wafers were used as substrates. The temperature during deposition was the ambient temperature. The substrates were placed on a carrier and transported with constant speed, passing the activated twin magnetron arrangement horizontally several times until the desired layer thickness was reached.

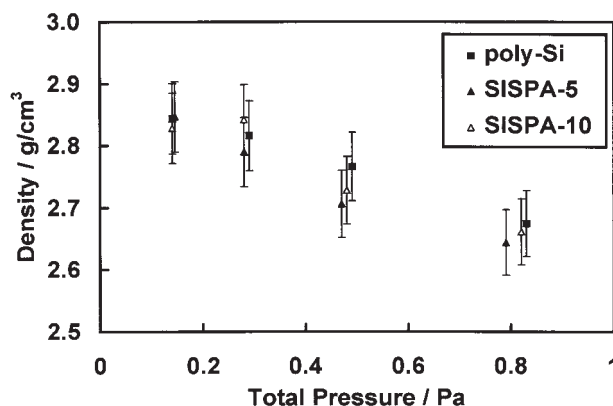


Fig. 3. Density of  $\text{Si}_3\text{N}_4$  layers deposited at different total pressures with different target materials.



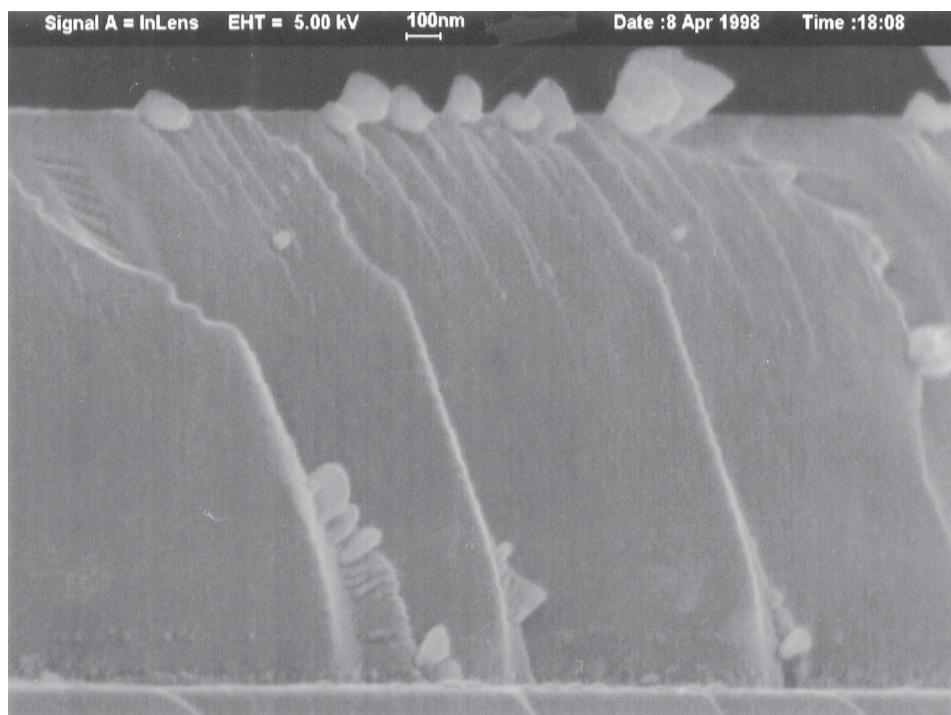


Fig. 4. SEM picture of the cross section of a Si<sub>3</sub>N<sub>4</sub> layer deposited from a SISPA™ 10 alloy target at a pressure of 0.15 Pa.

The layer densities were determined by measuring the film thickness and the mass of the substrates before and after deposition with a micro balance with a resolution of 10 μg. The layer thickness was measured using the stylus method. The surface morphology and cross sections of the

layers were examined with scanning electron microscopy (SEM). The microhardness was determined with the indentation method using a Vickers diamond. The internal stress of the films was calculated using the film thickness and the radius of curvature of the Si wafers before and after deposi-

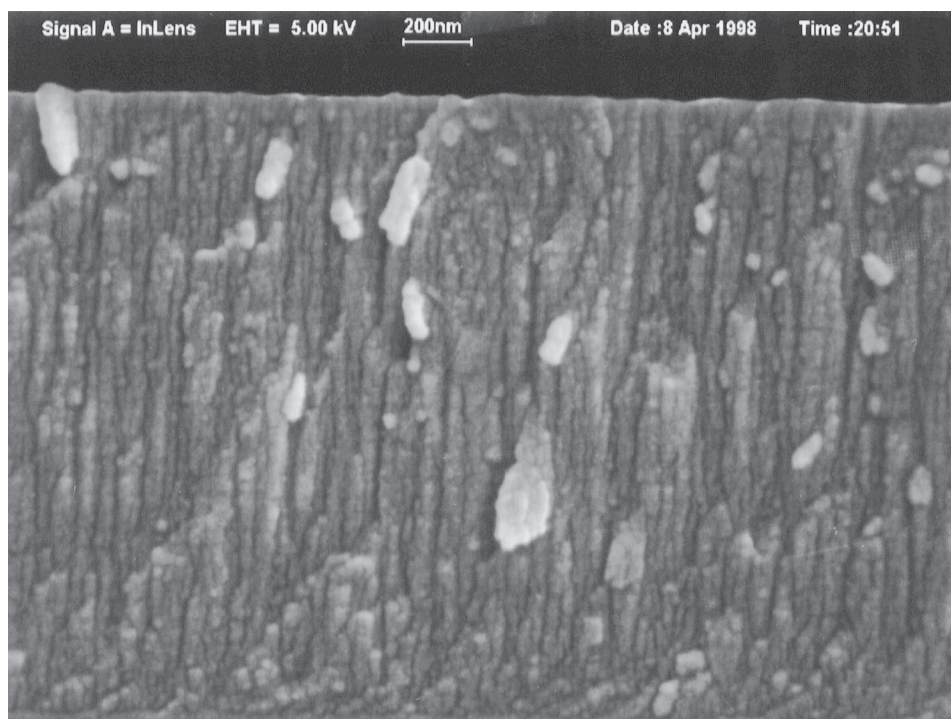


Fig. 5. SEM picture of the cross section of a Si<sub>3</sub>N<sub>4</sub> layer deposited from a SISPA™ 10 alloy target at a pressure of 1.10 Pa.

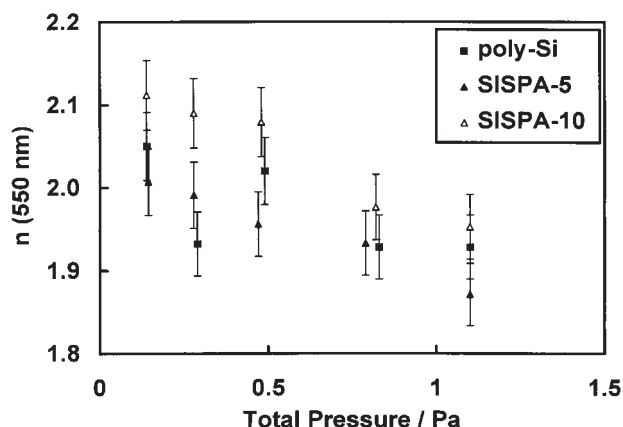


Fig. 6. Index of refraction for a wavelength of 550 nm of  $\text{Si}_3\text{N}_4$  layers deposited at different total pressures from different target materials.

tion. These examinations were carried out using samples with a film thickness of about 2  $\mu\text{m}$ . The index of refraction was determined by spectral ellipsometry (Sentech SE 800) using samples of about 150 nm film thickness.

### 3. Results

#### 3.1. $\text{Si}_3\text{N}_4$

The density of the deposited layers decreases in general with increasing total pressure (Fig. 3). For all target materials, the measured value ranges from 2.85  $\text{g}/\text{cm}^3$  at 0.15 Pa to about 2.65  $\text{g}/\text{cm}^3$  at 1.1 Pa. This behavior is typical for sputter deposited layers and can be attributed to a change in the structure. At higher total pressures, the sputtered particles are scattered. The deposition rate is lower and particles arrive at the substrate with lower energy and a high oblique component, thus changing the growth mechanisms and the morphology of the layer. SEM pictures of a cross section of a  $\text{Si}_3\text{N}_4$  layer deposited at low and high total pressure using a SISPA™ 10 target are shown in Figs. 4 and

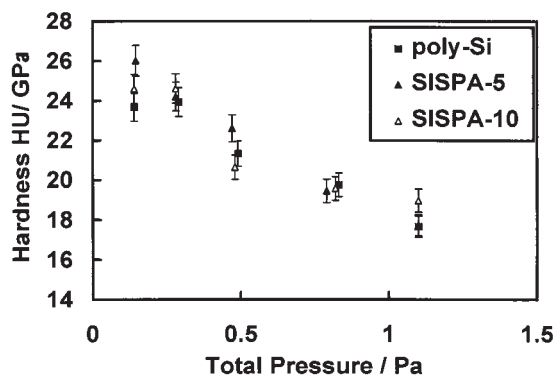


Fig. 7. Microhardness of  $\text{Si}_3\text{N}_4$  layers deposited at different total pressures from different target materials.

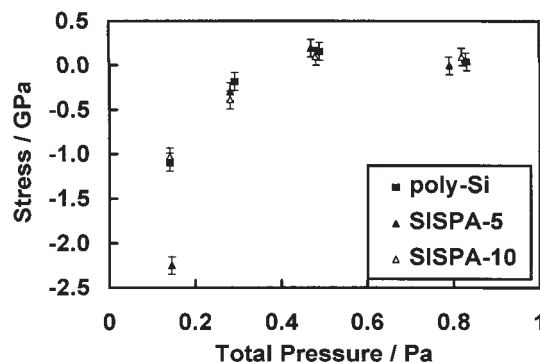


Fig. 8. Internal stress of  $\text{Si}_3\text{N}_4$  layers deposited at different total pressures for different target materials.

5, respectively. A transition from a homogeneous structure to a fibrous morphology can be seen. This is similar for the other target materials used in this work.

According to the density, the index of refraction measured for a wavelength of 550 nm decreases for increasing total pressures (Fig. 6). For the high purity poly-Si target, the value ranges from about 2.05 to 1.93, which is typical for plasma-deposited  $\text{Si}_3\text{N}_4$  [8]. Layers which were deposited using the SISPA™ 5 targets show almost the same values, but a clear increase of the index of refraction can be seen for the SISPA™ 10 target, perhaps due to an increasing AlN content in the layer.

Also the microhardness of the deposited layers decreases with increasing total pressure due to the changing density and morphology (Fig. 7). The values are significantly higher than for uncoated slide glass and range from 25–18 GPa. The mechanical stability of layer systems can be improved if this material is used as the top layer. There is no clear dependency on the target material.

The internal stress of the deposited layers depends very strongly on the total pressure (Fig. 8). High values of compressive stress are measured for low total pressures up to about 0.4 Pa. The stress can be reduced by increasing the total pressure. Then it turns to the tensile region. Care has to be taken if conclusions are drawn for optical layer systems

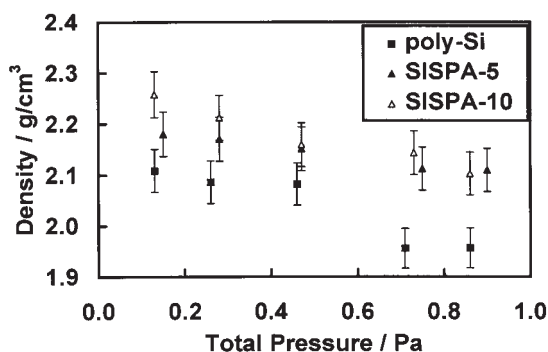


Fig. 9. Density of  $\text{SiO}_2$  layers deposited at different total pressures with different target materials.

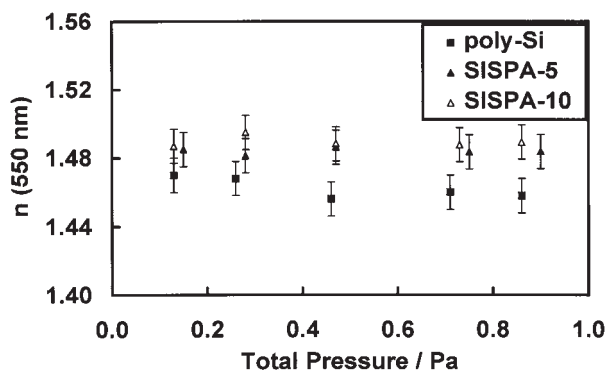


Fig. 10. Index of refraction for a wavelength of 550 nm of  $\text{SiO}_2$  layers deposited at different total pressures from different target materials.

because film thicknesses in such systems are much lower. The measured values do not only include the intrinsic stress due to the layer structure, but also the thermal stress due to different thermal expansion coefficients of the film and the substrate. As can be seen, there is no large difference between the different target materials.

### 3.2. $\text{SiO}_2$

As shown in Fig. 9, the density of the deposited layers decreases in general with increasing total pressure. For the films deposited using the conventional poly-Si target, the value ranges from about 2.10–1.95  $\text{g/cm}^3$ . The reasons for this are similar to the ones for  $\text{Si}_3\text{N}_4$ . Interestingly, the density is higher for the alloy targets. The layers reach values up to 2.25  $\text{g/cm}^3$  at a total pressure of 0.15 Pa.

The obtained indices of refraction for a wavelength of 550 nm as a function of total pressure are shown in Fig. 10. Only the layers deposited with a poly-Si target show a slight decrease from about 1.47 to 1.46 with increasing pressure as expected because of the decreasing density of the layer. The layers using alloy targets have a slightly higher index of refraction of about 1.48 to 1.49. This can

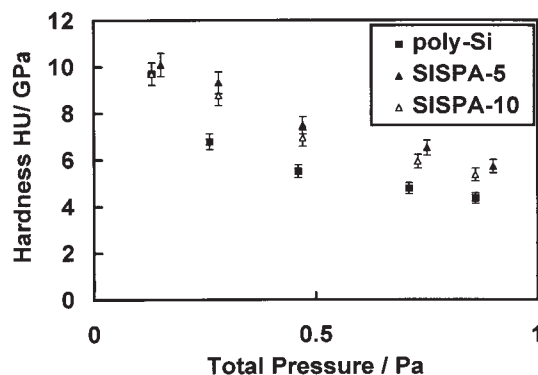


Fig. 11. Microhardness of  $\text{SiO}_2$  layers deposited at different total pressures from different target materials.

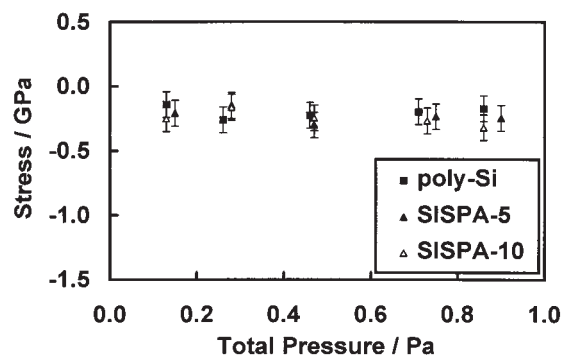


Fig. 12. Internal stress of  $\text{SiO}_2$  layers deposited at different total pressures for different target materials.

be due to the  $\text{Al}_2\text{O}_3$  content and the higher density. A dependency on the pressure was not detected.

The microhardness of the deposited layers decreases with increasing total pressure (Fig. 11). For the lowest total pressures, layers from poly-Si targets reach values of uncoated slide glass, which is about 8 GPa. This value decreases to about 4 GPa at 0.9 Pa. This change correlates with the change in density and structure. The hardness values for layers from alloy targets are slightly higher. This can be due to the higher density of these layers.

The determined stress values were very low. For all target materials, a compressive stress of about  $-0.2$  GPa was measured. This value was independent of the total pressure (Fig. 12).

## 4. Conclusions

Casted Si/Al alloy targets can be used to replace the more expensive high purity boron-doped poly-Si targets. A reduced brittleness of the material and the possibility to produce larger tile sizes and different shapes are important advantages. The  $\text{Si}_3\text{N}_4$  and  $\text{SiO}_2$  layer properties are not very different from the ones when pure Si targets are used. The density is similar for  $\text{Si}_3\text{N}_4$  and slightly higher for  $\text{SiO}_2$ . The index of refraction of refraction changes only slightly due to the different density and the Al content. The morphology shows the same dependency on the total pressure and also the values for the internal stress are almost identical.

Si/Al alloy targets of the SISPA™ type are already successfully used in industrial production lines for low emissivity coatings and may replace poly-Si targets in the near future completely.

## References

- [1] G. Bräuer, J. Szczyrbowski, G. Teschner, J. Non-Cryst. Solids 218 (1997) 19.
- [2] J. Szczyrbowski, G. Teschner, Soc. Vac. Coaters, Proc. 38th Annu. Tech. Conf. (1995) 380.

# Explore Litigation Insights

Docket Alarm provides insights to develop a more informed litigation strategy and the peace of mind of knowing you're on top of things.

## Real-Time Litigation Alerts



Keep your litigation team up-to-date with **real-time alerts** and advanced team management tools built for the enterprise, all while greatly reducing PACER spend.

Our comprehensive service means we can handle Federal, State, and Administrative courts across the country.

## Advanced Docket Research



With over 230 million records, Docket Alarm's cloud-native docket research platform finds what other services can't. Coverage includes Federal, State, plus PTAB, TTAB, ITC and NLRB decisions, all in one place.

Identify arguments that have been successful in the past with full text, pinpoint searching. Link to case law cited within any court document via Fastcase.

## Analytics At Your Fingertips



Learn what happened the last time a particular judge, opposing counsel or company faced cases similar to yours.

Advanced out-of-the-box PTAB and TTAB analytics are always at your fingertips.

## API

Docket Alarm offers a powerful API (application programming interface) to developers that want to integrate case filings into their apps.

## LAW FIRMS

Build custom dashboards for your attorneys and clients with live data direct from the court.

Automate many repetitive legal tasks like conflict checks, document management, and marketing.

## FINANCIAL INSTITUTIONS

Litigation and bankruptcy checks for companies and debtors.

## E-DISCOVERY AND LEGAL VENDORS

Sync your system to PACER to automate legal marketing.